Energetics and Affinity of the Histone Octamer for Defined DNA Sequences†

Joel M. Gottesfeld*,‡ and Karolin Luger§

Department of Molecular Biology, The Scripps Research Institute, La Jolla, California 92037, and Department of Biochemistry and Molecular Biology, Colorado State University, Fort Collins, Colorado 80523

Received May 15, 2001; Revised Manuscript Received July 18, 2001

ABSTRACT: Previous studies have compared the relative free energies for histone octamer binding to various DNA sequences; however, no reports of the equilibrium binding affinity of the octamer for unique sequences have been presented. It has been shown that nucleosome core particles (NCPs) dissociate into free DNA and histone octamers (or free histones) on dilution without generation of stable intermediates. Dissociation is reversible, and an equilibrium distribution of NCPs and DNA is rapidly attained. Under low ionic strength conditions (<400 mM NaCl), NCP dissociation obeys the law of mass action, making it possible to calculate apparent equilibrium dissociation constants (K_ds) for NCPs reconstituted on defined DNA sequences. We have used two DNA sequences that have previously served as model systems for nucleosome reconstitution studies, human α-satellite DNA and *Lytechinus variegatus* 5S DNA, and find that the octamer exhibits K_ds of 0.03 and 0.06 nM, respectively, for these sequences at 50 mM NaCl. These DNAs form NCPs that are ∼2 kcal/mol more stable than total NCPs isolated from cellular chromatin. As for mixed-sequence NCPs, increasing ionic strength or temperature promotes dissociation. van't Hoff plots of K_as versus temperature reveal that the difference in binding free energy for α-satellite and 5S NCPs compared to bulk NCPs is due almost entirely to a more favorable entropic component for NCPs formed on the unique sequences compared to mixed-sequence NCPs. Additionally, we address the contribution of the amino-terminal tail domains of histones H3 and H4 to octamer affinity through the use of recombinant tailless histones.

The template for gene transcription, DNA replication, and repair is the nucleoprotein complex known as chromatin. At the first level of chromatin organization, two superhelical turns of DNA (147 base pairs in length) are wrapped around a disk-shaped octamer of the core histones (containing two copies each of H2A, H2B, H3, and H4) to form the nucleosome core particle (NCP) (*1*). An additional 20−80 bp of linker DNA extends from the NCP and binds the linker histone H1 to form the fundamental repeating unit of chromatin, the nucleosome. Nucleosomes are subject to multiple higher order levels of organization, which are aided by the linker histone H1. The 2.8 Å crystal structure of the NCP provides a detailed view of the structure of the histone proteins, nucleosomal DNA, and histone−DNA contacts (*2*). However, this snapshot of the nucleosome does not reveal the energetics of this DNA−protein complex, nor does it explain possible subtle differences in structure that would occur with different DNA sequences, or as a consequence of postsynthetic modifications of the core histones.

The histone octamer is often found to occupy single or limited numbers of translational positions with respect to the underlying DNA sequence, especially on promoter DNA sequences [reviewed in (*1, 3, 4*)]. Since nucleosomes affect the availability of DNA for interaction with transcription factors and other components of the nuclear environment [see (*5, 6*) and references cited therein], it is important to investigate the interaction of the histone octamer with defined DNA sequences, such as gene promoters and mRNA-coding sequences. Additionally, changes in histone modification states, such as acetylation (*7, 8*), may directly affect nucleosome structure and the ability of chromatin domains to be transcribed. Thus, a thorough understanding of the mechanisms of transcriptional activation will require detailed knowledge of nucleosome structure, stability, DNA accessibility, and the effects of postsynthetic modifications on these parameters.

Numerous studies have addressed the relative binding free energies of various DNA sequences for the histone octamer [(*4, 9, 10*) and references cited therein]. These experiments use a competition reconstitution protocol (*9*) to compare the relative affinities of various DNA sequences for the histone octamer. Differences in binding free energies can be calculated based on the extent of incorporation of different DNA sequences into NCPs compared to a standard reference DNA sequence. The range of observed free energy differences between the best to worst nucleosome-associating sequences is on the order of ∼2−3 kcal/mol (*4, 9*), corresponding to differences of no more than ∼100-fold. Additionally, this method has been applied to study the contribution of histone tails to NCP stability (*10*).

The apparent equilibrium dissociation constant (K_d) of the histone octamer for bulk nucleosomal DNA has been derived (*11*) based on the observation that nucleosomes dissociate into free DNA and histones on dilution [(*12, 13*) and

† This work was supported by grants from the National Institutes of Health (GM57148 to J.M.G. and GM61909 to K.L.).

* To whom correspondence should be addressed. E-mail address: joelg@scripps.edu.

‡ The Scripps Research Institute.

§ Colorado State University.

10.1021/bi0109966 CCC: $20.00
Published on Web 08/17/2001

references cited therein]. Yager and van Holde (*13*) and Ausio et al. (*11*) demonstrated that nucleosome dissociation on dilution is reversible, and increases with increasing salt concentration (and/or temperature) and decreasing particle concentration. Since NCP dissociation follows the law of mass action, an apparent K_d can be calculated based on particle concentration and the fraction of DNA in the NCP (*11*). This analysis has yielded K_d values in the low nanomolar range for bulk sequence NCPs at low (50−100 mM) NaCl concentrations. In contrast, to our knowledge, no measurements of the absolute binding affinity of the histone octamer for unique DNA sequences have been published. Here we use the NCP dilution method to determine octamer binding affinities for two unique DNA sequences, the 5S ribosomal RNA gene of the sea urchin *Lytechinus variegatus* (*14*) and human α-satellite DNA (*15*). These sequences have been used extensively as model systems to study histone octamer positioning, nucleosome assembly, and nucleosome structure. The α-satellite DNA sequence was used for determination of the crystal structure of the nucleosome (*2*). The differences in free energies that we observe for these unique sequences compared to bulk nucleosomal DNA are similar to the reported free energy differences using the competition reconstitution method (*4*, *9*). Importantly, the dilution method provides complimentary information to that obtained by the competitive reconstitution method, and by measuring K_ds as a function of incubation temperature, this method allows for an analysis of the thermodynamic processes (enthalpy and entropy) that drive binding reactions. We have also used the dilution method to assess the role of the amino-terminal tails of the core histones in octamer affinity. The method we describe provides a simple and reliable approach to determine the absolute binding affinities of various DNAs for the histone octamer and the effects of histone modifications on NCP affinities.

MATERIALS AND METHODS

Nucleosome Core Particles. NCPs were reconstituted on a 146 bp palindromic DNA fragment derived by head to head ligation of the 73 bp human α-satellite DNA (*2*, *15*) and a 146 bp DNA fragment derived from *Lytechinus variegatus* 5S DNA (*16*). DNA was dephosphorylated with shrimp alkaline phosphatase (Roche Molecular Biochemicals) and was subsequently radiolabeled at its 5′ ends with T4 polynucleotide kinase (Roche) and [γ-^{32}P]ATP using standard protocols. Generally, 1.0 μg of DNA was mixed with 1.1 μg of preformed histone octamer, containing recombinant *Xenopus laevis* histones (*16*, *17*), yielding a 1:1 molar ratio of octamer to DNA, in 2 M NaCl, 10 mM Tris-HCl, pH 7.6, in a total volume of 10−12 μL. Other input ratios of octamers to DNA were used, and these values are given in the text and figure captions. Nucleosome reconstitution was performed by stepwise reduction of the ionic strength as described (*18*) using steps of 1, 0.8, 0.67, and 0.2 M NaCl. Each incubation was for 1 h at ambient temperature, followed by a 2 h incubation at 37 °C, as described (*17*). Incubation of the NCP reconstitute at 37 °C shifted the population of nucleosome positions on satellite DNA to a single unique position (*17*). The dilution buffer was 10 mM Tris-HCl, pH 7.6. Following the last incubation, the sample was diluted to 0.1 M NaCl and was stored at 4 °C for up to 2 weeks. NCPs were also reconstituted with octamers containing either the histone H3 globular domain (amino acids 27−135) or the H4 globular domain (amino acids 20−102), respectively, and the other full-length histones, or octamers containing only the globular domains of the histones (H2A amino acids 19−118; H2B amino acids 27−122; and the globular domains of H3 and H4 as described above) (*16*, *17*). An SDS−polyacrylamide gel of these histone proteins has been presented (*16*). Refolding and purification of these octamers were done as described for full-length histone octamer (*17*). Where indicated, NCPs were concentrated by microdialysis for 1 h using a Slide-A-Lyzer with a 10 000 MW cutoff and concentrating solution (catologue number 66527) from Pierce, according to the manufacturer's instructions.

Electrophoretic Mobility Shift Assays (EMSAs). The extent of nucleosome assembly was monitored by electrophoresis of aliquots of the reconstituted nucleosomes (diluted to ∼5 nM with 10 mM Tris-HCl, pH 7.6, 50 mM NaCl, 10% glycerol) on a 6% nondenaturing polyacrylamide gel (29:1 acrylamide to bis-acrylamide ratio) using 88 mM Tris−borate, pH 8.3, 2 mM EDTA (1× TBE) as the gel and electrophoresis buffer. The fraction of the DNA incorporated into core particles was determined by phosphorimage analysis of the dried gel using a Molecular Dynamics Phosphorimager SI with ImageQuant software. Generally, for wild-type core particles, 86−96% reconstitution was observed, and no change in the fraction of DNA in the core particle was noted on storage. At a 1:1 molar ratio of fully globular domain histone octamers to DNA, approximately 50−55% of the DNA was incorporated into NCPs, while at the 1.6:1 ratio, nearly 90% of the DNA was in the NCP. We note that a fraction of the input radioactivity in each sample is retained in the wells of the nondenaturing gels regardless of whether the sample is protein-free DNA or NCPs (see figures below). We have been unable to fully eliminate this material by the addition of nonionic detergents, bovine serum albumin, or excess carrier DNA to the samples. However, since similar percentages of input radioactivity are retained in the wells for both protein-free DNA and NCPs, this material can be ignored in K_d determinations.

K_ds were determined by serial dilution of the NCPs, ranging from 30 to 0.01 nM, using the following dilution buffer: 10 mM Tris-HCl, pH 7.6, 10% glycerol, 0.1% Igepal CA-630 (Sigma, previously known as NP-40), 500 μg/mL glycogen (10 μg/20 μL), and the concentrations of NaCl cited in the text and figure legends. Glycogen and Igepal were included to reduce nonspecific binding of the samples to the reaction tubes on dilution. Samples were incubated for sufficient time to reach the equilibrium distribution of DNA and NCPs and then subjected to nondenaturing gel electrophoresis on 6% gels (as above). Phosphorimage analysis was used to quantitate the fraction of DNA and NCPs at each dilution point. Data were plotted as fraction of NCP remaining (normalized to the fraction of NCP at 30 nM) versus concentration of free octamers, using a nonlinear least-squares fitting program (KaleidaGraph version 3.0.1, Abelbeck Software). To obtain K_ds, the data were fit to the Hill equation: fraction bound = $[\text{free octamer}]^n/([\text{free octamer}]^n + K_d^n)$, where n is the Hill coefficient. At low ionic strength (400 mM NaCl and below) and at 23 °C, similar quality fits to the data were obtained by fixing the Hill coefficient to 1.0 or allowing the Hill coefficient to be a floating variable. The concentration of free octamer was determined from the

fraction of DNA in core particles at each dilution point and the input concentrations of DNA and octamers, according to the relationship: [free octamer] = [octamer] × (1 − fraction NCP remaining).

RESULTS

Nucleosome Core Particle Reconstitution. NCPs were reconstituted on 146 bp DNA fragments derived from human α-satellite (*2, 15*) and *Lytechinus variegatus* 5S DNA (*14, 16*) with recombinant histones (*17*) using a salt dilution protocol (*18*). As demonstrated previously (*17*), the histone octamer adopts multiple positions on both of these DNA sequences. However, a heating step (2 h at 37 °C) shifts the population of nucleosome positions to a single unique position, as judged by nondenaturing gel electrophoresis [(*17*) and see figures below]. The stability of NCPs on both DNA sequences, and the integrity of the histones, was not affected by storage at 4 °C for several weeks (data not shown).

Determination of Apparent Dissociation Constants. Velocity sedimentation studies and EMSA have demonstrated that dilution of native NCPs results in dissociation of the core particle into free DNA and histones (*11*−*13*). To derive reliable dissociation constants from such an NCP dilution experiment, several criteria must be met: first, the extent of dissociation at a given NCP concentration must represent the equilibrium distribution of free DNA and histone octamers (or free histones) at that concentration, with no other intermediate species present; second, the process of dissociation must be reversible; and, third, the extent of dissociation must only depend on the concentration of NCPs (i.e., dissociation as a function of concentration can be described by a first-order equation). Naturally, solvent conditions and temperature will also affect the extent of dissociation (*11*−*13*). If these criteria are met, then apparent K_ds can be derived from the fraction of DNA in the NCP at various NCP concentrations (*11*). As for bulk nucleosomes prepared from cellular chromatin, NCPs reconstituted with either α-satellite or 5S DNA dissociate on dilution as judged by EMSA (Figure 1A,B). No other complexes are generated upon dissociation, suggesting that no stable intermediates (such as DNA plus tetramers of H3 + H4 or NCPs bound with an extra dissociated octamer) are generated and that dissociation proceeds from the NCP to free DNA plus free histones. Possible mechanisms of dissociation have been discussed previously (*11, 13*). Plots of the fraction of DNA in NCP versus free octamer concentration yield simple isotherms that can be fit to the Hill equation, with Hill coefficients of 1.0 (Figure 1C). Thus, dissociation appears to depend simply on NCP concentration.

Based on several independent experiments, we find that the apparent K_ds for the α-satellite and 5S NCPs are 0.03 and 0.06 nM, respectively, at 50 mM NaCl (Figure 1A−C, Table 1). These values correspond to a free energy difference of +0.42 kcal/mol between the α-satellite and 5S sequences (Table 1). As an independent verification of the relative differences in octamer affinity for these DNA sequences, we compared the extent of reconstitution on each of these DNAs using the competition reconstitution method of Shrader and Crothers (*9*). In this experiment, 0.1 μg of radiolabeled α-satellite or 5S DNA was mixed with 0.9 μg of unlabeled α-satellite DNA and used for reconstitution with various

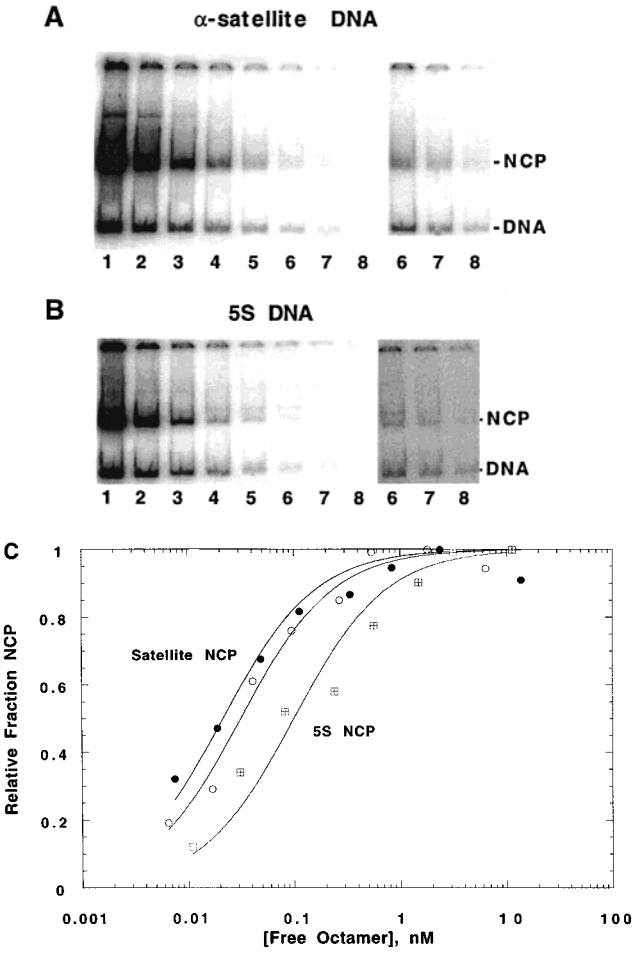

FIGURE 1: Determination of binding affinities of the histone octamer for (A) α-satellite and (B) 5S DNA by serial dilution of NCPs in steps of 30, 10, 3.34, 1.12, 0.38, 0.13, 0.042, and 0.014 nM (lanes 1−8, respectively) in buffer containing 50 mM NaCl. After a 3 h incubation at 23 °C ambient temperature, the samples were analyzed on 6% nondenaturing gels, and the fraction of DNA in NCPs in each lane was determined by phosphorimage analysis. Longer exposures for lanes 6−8 are shown on the right. NCPs were reconstituted as described under Materials and Methods. The minor band that migrates slower than the α-satellite NCP (panel A) could represent NCPs with an additional octamer; however, the identity of this species has not been determined. (C) The fraction of DNA in the NCP, relative to the 30 nM sample, is plotted versus the concentration of free octamer. Free octamer concentration was determined as described under Materials and Methods. α-Satellite NCPs were incubated for 3 h (open circles) or 24 h (filled circles) prior to electrophoresis, and 5S NCPs (squares) were incubated for 3 h. The double bands in the 5S NCP (see lanes 4, 6, and 7) could represent multiple translational positions of the octamer on this DNA (*16, 17*).

amounts of octamers. At an approximate 0.6:1 input ratio of octamer to DNA, 68% of the radiolabeled α-satellite DNA was incorporated into NCPs, while under identical conditions, 50% of the labeled 5S DNA was incorporated into NCPs (Figure 2). This ratio of incorporation reflects a +0.45 kcal/mol difference in binding free energies ($\Delta\Delta G°$) between these two DNA sequences [Table 2 and (*9*)], in agreement with the +0.42 kcal/mol difference found by the dilution method.

Control experiments were performed to address the issues of equilibrium and reversibility. To ensure that equilibrium is reached in our experiments, we monitored the distribution of NCP and DNA at various NCP concentrations as a

Table 1: NCP Binding Affinities and Free Energies

NCP	[NaCl] (mM)	app equilibrium binding affinity (K_d, nM)[a]	$-\Delta G°$ (kcal/mol)[b]	$\Delta\Delta G°$ (kcal/mol)[c]
α-Sat	50	0.030 ± 0.005 ($N = 6$)	14.25	0
α-Sat	100	0.08 ± 0.01 ($N = 2$)	13.68	+0.58
α-Sat/H3 globular	50	0.09 ± 0.02 ($N = 4$)	13.60	+0.65
α-Sat/H4 globular	50	0.08 ± 0.01 ($N = 4$)	13.67	+0.58
α-Sat/globular	50	0.15 ($N = 1$)	13.31	+0.94
5S DNA	50	0.06 ± 0.02 ($N = 3$)	13.83	+0.42
5S DNA/globular	50	0.40 ($N = 1$)	12.73	+1.10
bulk[d]	50	1.2	12.08	+2.17
bulk[e]	100	3.6	11.44	+2.54

[a] Determined by EMSA by dilution. Mean values and standard deviations for the number of determinations (N) are given. [b] Calculated according to the equation: $\Delta G° = -RT \ln K_a$, where $T = 296$ K (23 °C) and $R = 1.987$. [c] $\Delta\Delta G°$ values calculated by comparing $\Delta G°$s at equivalent NaCl concentrations. [d] Data from Cotton and Hamkalo (*12*) for mouse L929 cell core particles, as calculated by Ausio et al. (*11*). [e] Data from Ausio et al. (*11*) for chicken erythrocyte core particles.

Table 2: NCP Free Energies Determined by Dilution Compared to Competitive Reconstitution

NCP	$\Delta\Delta G°$ dilution method (kcal/mol)[a]	$\Delta\Delta G°$ reconstitution method (kcal/mol)[b]
α-Sat/WT octamer	0	0
5S DNA/WT octamer	+0.42	+0.45
α-Sat/H3 globular	+0.65	+0.59
α-Sat/H4 globular	+0.58	+0.68
α-Sat/globular	+0.94	+0.93
5S DNA/globular	+1.10	+1.12

[a] From Table 1. [b] Calculated from the fraction of DNA incorporated into NCPs at equivalent molar ratios of the indicated octamer to each DNA as described by Widlund et al. (*10*).

function of incubation time. In agreement with previous studies (*12*), we find that dissociation is very rapid, even at low ionic strength. At subnanomolar NCP concentrations and 50 mM NaCl, no significant change in the fraction of NCPs was found between 30 min and 28 h (data not shown). Figure 1C also compares the results of dissociation experiments in which α-satellite NCPs were incubated for either 3 or 24 h at ambient temperature prior to electrophoresis. Within experimental error, similar K_ds were obtained for the α-satellite NCPs under both conditions (0.03 and 0.02 nM at 3 and 24 h, respectively), demonstrating that equilibrium is indeed attained after a 3 h incubation.

To address reversibility, we diluted the α-satellite NCP to 0.5 nM in buffer containing 200 mM NaCl and, after incubation at ambient temperature for 2 h, analyzed an aliquot by EMSA. Under these conditions, the fraction of DNA in the NCP is 0.12, compared to 0.86 for a sample analyzed at 6 nM (data not shown). When the 0.5 nM sample (188 μL) was concentrated approximately 13-fold (to ~6 nM in ~14 μL) prior to EMSA, the fraction of DNA in the NCP increased to 0.75. Thus, in agreement with previous studies (*13*), reassociation of the NCP demonstrates that dissociation by dilution is reversible.

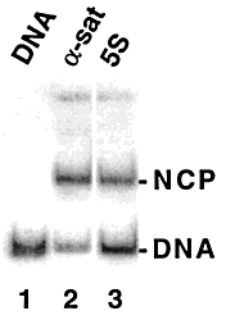

FIGURE 2: Extent of incorporation of α-satellite and 5S DNAs into NCPs, as determined by nondenaturing gel electrophoresis. NCP reconstitution was performed as described under Materials and Methods except the reactions contained 0.1 μg of the indicated radiolabeled DNA and 0.9 μg of unlabeled α-satellite DNA along with a 0.6:1 weight ratio of histone octamers to DNA. Reconstitutes were analyzed at a concentration of 3 nM (at 50 mM NaCl), which is above the concentration range where NCP dissociation occurs (Figure 1).

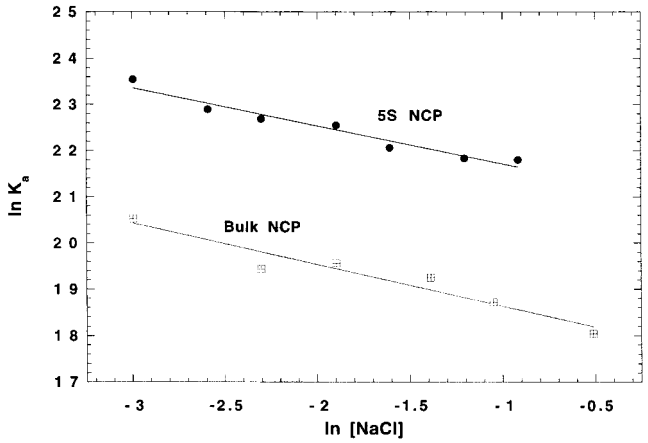

FIGURE 3: Double-logarithmic plot of equilibrium association constant versus ionic strength. Data for 5S NCPs are from this study while the data for bulk nucleosomes were taken from Cotton and Hamkalo (*12*) as analyzed by Ausio et al. (*11*).

Effect of NaCl Concentration on Apparent Dissociation Constants. As previously observed by several groups, the extent of NCP dissociation increases with increasing ionic strength [(*11*) and references cited therein]. We determined the apparent K_d for 5S and α-satellite NCPs as a function of NaCl concentration and found, as expected, that the K_d increased with increasing NaCl concentrations. Plots of $-\ln K_a$ versus ln [NaCl] yield straight lines for both our current data for 5S NCPs and previous data for bulk nucleosomes isolated from L929 cells [Figure 3, (*11, 12*)]. Similar results were obtained with α-satellite NCPs (data not shown). The slope of such a double-log plot should yield the number of ion pairs formed in the octamer−DNA interaction (*11*, *19*, *20*). Surprisingly, however, far smaller values are obtained for each of the NCPs (0.8−1.1) than would be expected based on the numerous basic amino acid−DNA phosphate contacts observed in the crystal structure of the NCP (*2*). The finding that these slopes correspond to approximately one ion pair per NCP suggests that DNA counterion release on formation of ionic interactions in the NCP is largely offset by ion uptake due to shielding of adjacent phosphates on the two gyres of DNA in the NCP (*2*).

Effect of Temperature on Apparent Dissociation Constants. K_ds for both α-satellite and 5S NCPs were determined by

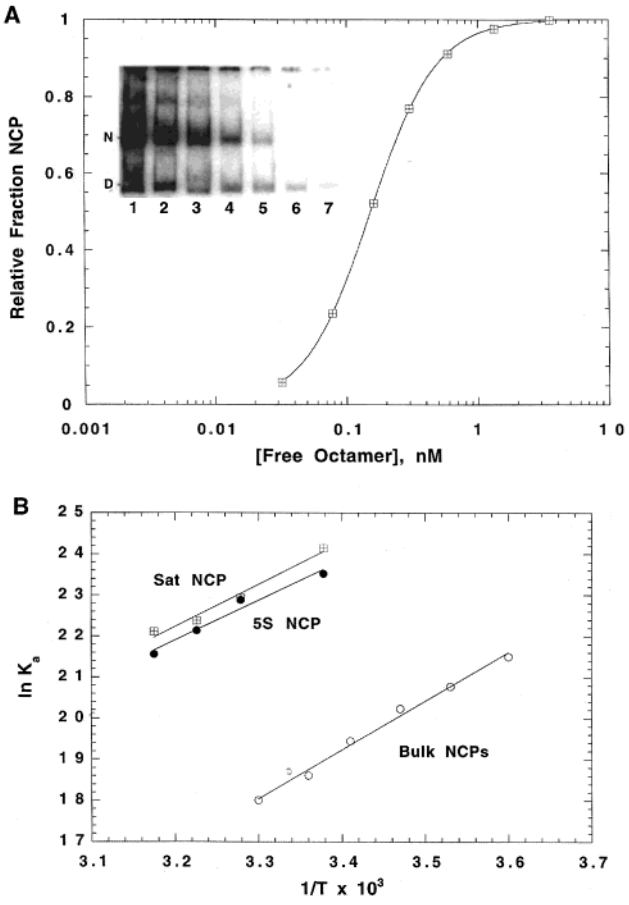

FIGURE 4: Temperature dependence of the K_ds for α-satellite and native NCPs. (A) Dilution experiment for α-satellite NCPs performed by incubating samples in buffer containing 50 mM NaCl at 37 °C for 3 h prior to electrophoresis. A phosphorimage of the gel is shown as an inset. In lanes 1−7, the input concentrations of NCPs were 23, 7.7, 2.6, 0.86, 0.29, 0.10, and 0.03 nM, respectively. (B) van't Hoff plots of ln K_a versus 1/temperature (in kelvin) for α-satellite, 5S, and bulk NCPs. Data for bulk NCPs were taken from Ausio et al. (*11*).

Table 3: Temperature Dependence of K_ds

	app dissociation constants (nM)[a]	
temp (°C)	α-satellite NCP	5S NCP
23	0.03	0.06
32	0.11	0.12
37	0.19	0.24
42	0.25	0.44

[a] Determined by EMSA using the dilution method at 50 mM NaCl.

the dilution method as a function of temperature. In agreement with results with mixed-sequence nucleosomes (*11, 12*), the observed K_d increases with increasing temperature (Table 3). For example, at 37 °C and 50 mM NaCl, a $K_d = 0.19$ nM for the α-satellite NCP was obtained, compared to 0.03 nM at 23 °C (Figure 4A). Cooperativity in the dissociation profile is observed at 37 °C and above (Hill coefficients >1, Figure 4A). The basis for this cooperativity will require further investigation but could represent a structural transition in the histone octamer at these temperatures. Since the pH of Tris-buffered solutions decreases as a function of increasing temperature, it was important to show that any observed changes in K_d with increasing temperature are not due to effects of pH on NCP stability. At 42 °C, the pH of our standard EMSA buffer decreases to about 6.0. We therefore used EMSA to compare the fraction of DNA in NCPs at pH 6.0 (in 10 mM sodium cacodylate buffer, 50 mM NaCl, 0.1% Igepal, 10% glycerol) with that of the same sample at pH 7.6, and found no significant difference (data not shown). Thus, the observed decrease in binding affinity with increasing temperature is not due to an effect of pH on NCP integrity or stability.

Table 4: Enthalpic and Entropic Components of NCP Free Energies

NCP	$-\Delta G°$ at 23 °C (kcal/mol)[a]	$-\Delta H°$ (kcal/mol)[b]	$\Delta S°$ at 23 °C (cal/mol)[c]
α-Sat/WT octamer	14.25	20.39	20.7
5S DNA/WT octamer	13.83	19.29	18.5
native NCPs	12.08	23.64	39.1

[a] From Table 1. [b] Calculated from the slopes of the van't Hoff plots (shown in Figure 4B), where slope $= -\Delta H°/R$ (where $R = 1.987$). [c] Calculated according to $-\Delta G° = -\Delta H° + T\Delta S°$.

Based on the thermodynamic relationship between free energy and temperature, $\Delta G°$ values derived from the observed K_ds can be dissected into enthalpic and entropic contributions from a van't Hoff plot of ln K_a versus the inverse of temperature (in kelvin). Such plots for α-satellite, 5S, and bulk NCPs (*11*) yield straight lines with similar slopes (Figure 4B). $\Delta H°$ and $\Delta S°$ values can be derived from these slopes, and for each of the NCPs, similar $\Delta H°$ values are obtained (ranging from −19.3 to −23.6 kcal/mol, Table 4). For each NCP, $\Delta H°$ is more favorable (more negative) than the observed $\Delta G°$ at 23 °C, indicating that binding free energies are reduced by an unfavorable $\Delta S°$ component. Since each of the NCPs exhibits comparable enthalpies, the difference in $\Delta G°$ (and hence in K_d) between α-satellite and 5S NCPs compared to mixed-sequence NCPs is due almost entirely to a more favorable (formally, less unfavorable) entropic contribution to the overall binding free energy of these DNAs for the histone octamer. Since the histone octamer is the same for α-satellite and 5S NCPs, the observed difference in $\Delta S°$ must be due to a difference in the DNA, such as the intrinsic curvature of satellite DNA compared to 5S and mixed-sequence DNA. This issue is addressed below (see Discussion).

Role of Histone Amino-Terminal Tails in NCP Affinity and Stability. Apparent K_ds for α-satellite NCPs containing the globular domain of either histone H3 (amino acids 27−135) or histone H4 (amino acids 20−102) and the other full-length histones were determined both by the dilution method (Table 1) and by comparing the extent of reconstitution by EMSA (Figure 5). Apparent K_ds of ∼0.1 nM were obtained for these NCPs at 50 mM NaCl (Table 1), suggesting that the H3 and H4 amino-terminal tails each provide approximately −0.5 to −0.6 kcal/mol of binding free energy to the octamer/α-satellite DNA interaction. Comparison of the extent of NCP reconstitution at various ratios of H3- or H4-tailless octamers to DNA with wild-type NCPs also yields similar differences in free energies for these octamers versus wild-type octamers for α-satellite DNA (Figure 5 and Table 2).

Octamers containing only the globular domains of the histones (H2A amino acids 13−119; H2B amino acids 24−122; H3 and H4 as above) were also prepared and used for reconstitution on both α-satellite and 5S DNA (Figure 6). At a 1:1 molar ratio of globular domain histone octamers to α-satellite DNA, only approximately 50% of the DNA is

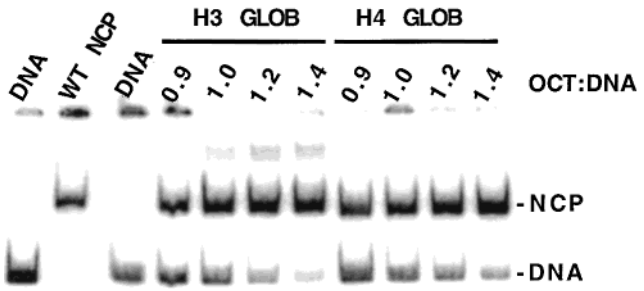

FIGURE 5: Extent of incorporation of α-satellite DNA into NCPs reconstituted with wild-type octamers (WT) or octamers containing the globular domains of histones H3 (amino acids 27−135) or H4 (amino acids 20−102), and the other full-length histones (denoted H3 GLOB and H4 GLOB, respectively). The input molar ratios of histone octamers to DNA are indicated in the figure. Reconstitutes were analyzed at a DNA concentration of 5 nM by electrophoresis on a 6% nondenaturing gel.

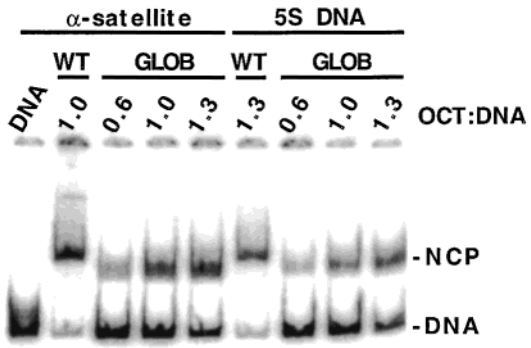

FIGURE 6: Reconstitution of α-satellite and 5S DNAs into NCPs with globular domain histones (denoted GLOB), as determined by 6% nondenaturing gel electrophoresis. The input molar ratios of histone octamers to DNA are indicated in the figure. WT denotes octamers containing full-length, wild-type histones. Reconstitutes were analyzed at a DNA concentration of 5 nM.

incorporated into NCPs. A similar result was obtained for 5S DNA at a 1.3:1 ratio (Figure 6). These results suggest a +0.9 to 1.1 kcal/mol difference in binding free energy of the globular domain octamers compared to wild-type octamers for α-satellite and 5S DNA (Table 2); however, these values should be viewed with caution since we do not have an accurate extinction coefficient for determining the concentration of the globular domain octamers. Nonetheless, these values are quite similar to those obtained with tailless histone octamers where proteolysis was used to remove histone tail domains (*10*). Similarly, when we performed dilution experiments with α-satellite or 5S NCPs containing the globular domain histones, K_d values commensurate with these free energy differences were obtained (Figure 7A−C, Tables 1 and 2). We note that longer incubation times are required for globular domain NCPs to reach equilibrium than the wild-type NCPs (data not shown). This may reflect a longer half-life for these NCPs compared to NCPs containing full-length histones. However, once equilibrium is attained, both the dilution and the extent of reconstitution methods yield similar differences in free energies for globular domain octamers compared to wild-type octamers (Table 2).

DISCUSSION

Several lines of evidence suggest that the K_d values we obtain by the dilution method are reliable estimates of the equilibrium binding affinity of the histone octamer for the

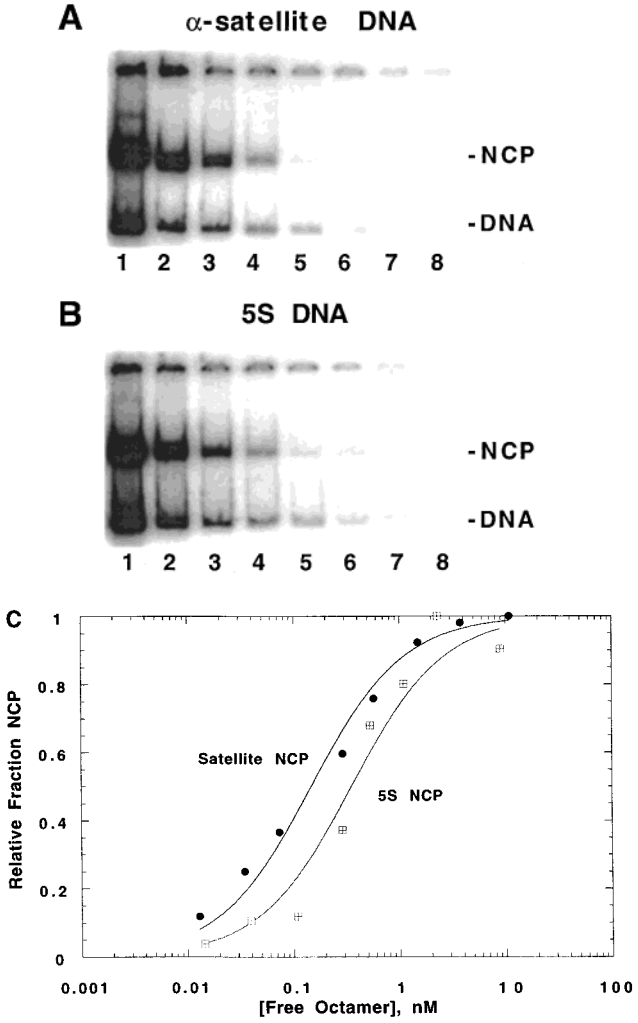

FIGURE 7: Dilution of α-satellite NCPs (A) and 5S NCPs (B) containing globular domain histones. The dilution experiment and analysis were identical to those in Figure 1 except samples were incubated for 20 h prior to electrophoresis. (C) The fraction of DNA in the NCP, relative to the 30 nM sample, is plotted versus the concentration of free octamer for α-satellite NCPs (circles) or 5S NCPs (squares) containing globular domain histone octamers.

selected DNA sequences we have investigated. First, different K_ds are obtained for two different DNA sequences, and the free energy difference for NCP formation between these sequences as calculated from these K_ds is similar to that obtained by the competitive reconstitution method [Table 2 and (*9*)]. Second, at low ionic strength (<400 mM NaCl) and ambient temperature, dissociation is dependent only upon NCP concentration; that is, dissociation can be described by a first-order equation with a Hill coefficient of 1.0 (Figure 1C). Third, on dilution, the sample rapidly reaches a stable equilibrium distribution of NCP and free DNA. If some process other than mass action promoted dissociation, then dissociation would increase with time until no NCPs remained; however, this is not the case. Fourth, dissociation is reversible, indicating that the constituents of the NCP are free in solution after dissociation.

We find a striking similarity between the free energy differences ($\Delta\Delta G°$s) derived by the dilution method with $\Delta\Delta G°$s derived from the competitive reconstitution method (Table 2). From the data presented by Cotton and Hamkalo (*12*), Ausio et al. (*11*) calculated a K_d of 1.2 nM for bulk

nucleosomes at 50 mM NaCl. This value corresponds to $\Delta\Delta G°$s of +2.2 and +1.8 kcal/mol for bulk NCPs compared to α-satellite and 5S NCPs, respectively (Table 1). A +1.6 kcal/mol free energy difference was obtained for bulk mononucleosomal DNA (~250 bp) compared to the *Lytechinus variegatus* 5S sequence (207 bp) by the competitive reconstitution method (*9*). The small difference in $\Delta\Delta G°$s between our current estimate and that reported previously is likely due to differences in DNA lengths and ionic conditions used in the two sets of experiments (*9*). Based on these comparisons and the arguments above, it is likely that the K_ds determined by the dilution method reflect reliable estimates of the binding affinities of the histone octamer for the α-satellite and 5S DNA sequences.

Additionally, K_ds determined by the dilution method will be useful to assess the effects of histone modifications on NCP affinities. We find that either the H3 tail or the H4 tail imparts a −500 cal/mol higher affinity of the histone octamer for α-satellite DNA, while all of the histone tails provide a −900 to −1100 cal/mol higher affinity for both 5S and α-satellite NCPs (Figures 6 and 7, Table 2). In a previous study, proteolysis was used to remove histone tails, and relative binding affinities were calculated based on the extent of reconstitution on various DNA sequences (*10*). In that study, tail domains imparted a −900 cal/mol higher affinity for straight or curved DNA sequences compared to proteolyzed histones. Tail domains had smaller effects on bent or intrinsically flexible DNAs. Thus, our results are in close agreement with these previous measurements. One observation concerning fully tailless histones that we note is that NCPs containing these histones take longer to reach the equilibrium extent of dissociation on dilution. This suggests that NCPs containing tailless octamers have a longer half-life (are more stable?) than NCPs containing full-length histones. However, at equilibrium, the K_d measured for tailless NCPs reflects the same free energy difference with wild-type NCPs as measured by extent of reconstitution (Table 2). The basis for this apparent difference in half-life will require further investigation.

Finally, from the temperature dependence of NCP affinity, enthalpic and entropic contributions to the observed binding free energies can be derived (Figure 4B, Table 4). Within the accuracy of our methods, each of the NCPs have similar enthalpic contributions to binding free energy, likely reflecting similar histone−DNA interactions in these NCPs. Previous studies have established that DNA bendability results in lower free energies for nucleosome formation [(*4*, *9*) and references cited therein]. However, DeSantis and colleagues have argued that curvature-dependent DNA hydration plays a role in sequence-dependent nucleosome stability (*21*, *22*). Numerous studies have also addressed the issue of DNA sequence periodicities of nucleosomal DNA and whether such periodicities influence DNA structure (bending/flexibility) and octamer affinity [see (*23*) and references cited therein]. Whatever the molecular explanation for the higher affinity of α-satellite and 5S DNAs for the histone octamer compared to mixed-sequence DNA, our findings indicate that this increased affinity is due to a lower entropic cost for NCP formation than for bulk nucleosomes. Given the similarity in enthalpy values we find for each of the NCPs (Table 4), we predict that differences in affinity between various DNA sequences will be due to differences in the entropic cost for these sequences to bind the histone octamer.

ACKNOWLEDGMENT

We thank Drs. Donald Crothers, Ken van Holde, and Gary Felsenfeld for discussions and comments on the manuscript and J. Ehley and S. Ebbesen for technical assistance.

REFERENCES

1. van Holde, K. E. (1989) *Chromatin*, Springer-Verlag, New York.
2. Luger, K., Mader, A. W., Richmond, R. K., Sargent, D. F., and Richmond, T. J. (1997) *Nature 389*, 251−260.
3. Flaus, A., and Richmond, T. J. (1998) *J. Mol. Biol. 275*, 427−441.
4. Thastrom, A., Lowary, P. T., Widlund, H. R., Cao, H., Kubista, M., and Widom, J. (1999) *J. Mol. Biol. 288*, 213−229.
5. Polach, K. J., and Widom, J. (1996) *J. Mol. Biol. 258*, 800−812.
6. Cirillo, L. A., McPherson, C. E., Bossard, P., Stevens, K., Cherian, S., Shim, E. Y., Clark, K. L., Burley, S. K., and Zaret, K. S. (1998) *EMBO J. 17*, 244−254.
7. Krebs, J. E., and Peterson, C. L. (2000) *Crit. Rev. Eukaryotic Gene Expression 10*, 1−12.
8. Cheung, P., Tanner, K. G., Cheung, W. L., Sassone-Corsi, P., Denu, J. M., and Allis, C. D. (2000) *Mol. Cells 5*, 905−915.
9. Shrader, T. E., and Crothers, D. M. (1989) *Proc. Natl. Acad. Sci. U.S.A. 86*, 7418−7422.
10. Widlund, H. R., Vitolo, J. M., Thiriet, C., and Hayes, J. J. (2000) *Biochemistry 39*, 3835−3841.
11. Ausio, J., Seger, D., and Eisenberg, H. (1984) *J. Mol. Biol. 176*, 77−104.
12. Cotton, R. W., and Hamkalo, B. A. (1981) *Nucleic Acids Res. 9*, 445−457.
13. Yager, T. D., and van Holde, K. E. (1984) *J. Biol. Chem. 259*, 4212−4222.
14. Simpson, R. T., and Stafford, D. W. (1983) *Proc. Natl. Acad. Sci. U.S.A. 80*, 51−55.
15. Yang, T. P., Hansen, S. K., Oisi, K. K., Ryder, O. A., and Hamkalo, B. A. (1982) *Proc. Natl. Acad. Sci. U.S.A. 79*, 6593−6597.
16. Luger, K., Rechsteiner, T. J., Flaus, A. J., Waye, M. M., and Richmond, T. J. (1997) *J. Mol. Biol. 272*, 301−311.
17. Luger, K., Rechsteiner, T. J., and Richmond, T. J. (1999) *Methods Enzymol. 304*, 3−19.
18. Hayes, J. J., and Lee, K. M. (1997) *Methods 12*, 2−9.
19. Record, M. T., Lohman, T. M., and de Haseth, P. (1976) *J. Mol. Biol. 107*, 145−158.
20. Record, M. T., Ha, J.-H., and Fisher, M. A. (1991) *Methods Enzymol. 208*, 291−343.
21. Anselmi, C., Bocchinfuso, G., De Santis, P., Savino, M., and Scipioni, A. (1999) *J. Mol. Biol. 286*, 1293−12301.
22. Anselmi, C., Bocchinfuso, G., De Santis, P., Savino, M., and Scipioni, A. (2000) *Biophys. J. 79*, 601−613.
23. Stein, A., and Bina, M. (1999) *Nucleic Acids Res. 27*, 848−853.

BI0109966